Biochimica et Biophysica Acta 1817 (2012) 298–305

Contents lists available at SciVerse ScienceDirect

Biochimica et Biophysica Acta

journal homepage: www.elsevier.com/locate/bbabio

Generation, characterization and crystallization of a cytochrome c_1-subunit IV fused cytochrome bc_1 complex from *Rhodobacter sphaeroides*

Ting Su [a], Lothar Esser [b], Di Xia [b], Chang-An Yu [a], Linda Yu [a,*]

[a] Department of Biochemistry & Molecular Biology, Oklahoma State University, Stillwater, OK 74078, USA
[b] Laboratory of Cell Biology, Center for Cancer Research, National Cancer Institute, National Institutes of Health, Bethesda, MD20892, USA

ARTICLE INFO

Article history:
Received 22 April 2011
Received in revised form 17 October 2011
Accepted 18 October 2011
Available online 25 October 2011

Keywords:
Supernumerary subunit
Bacterial cytochrome bc_1 complex
Rhodobacter sphaeroides
Fusion protein

ABSTRACT

Cytochrome bc_1 complex catalyzes the reaction of electron transfer from ubiquinol to cytochrome *c* (or cytochrome c_2) and couples this reaction to proton translocation across the membrane. Crystallization of the *Rhodobacter sphaeroides* bc_1 complex resulted in crystals containing only three core subunits. To mitigate the problem of subunit IV being dissociated from the three-subunit core complex during crystallization, we recently engineered an *R. sphaeroides* mutant in which the N-terminus of subunit IV was fused to the C-terminus of cytochrome c_1 with a 14-glycine linker between the two fusing subunits, and a 6-histidine tag at the C-terminus of subunit IV (c_1-14Gly-IV-6His). The purified fusion mutant complex shows higher electron transfer activity, more structural stability, and less superoxide generation as compared to the wild-type enzyme. Preliminary crystallization attempts with this mutant complex yielded crystals containing four subunits and diffracting X-rays to 5.5 Å resolution.

1. Introduction

The cytochrome bc_1 complex from the photosynthetic bacterium *Rhodobacter sphaeroides* catalyzes electron transfer from ubiquinol to cytochrome c_2 in a cyclic photosynthetic electron transfer chain [1,2]. Oxidation of ubiquinol is coupled to the translocation of protons across the membrane to generate a pH gradient and membrane potential that are used for ATP synthesis. This bacterial complex contains four protein subunits with apparent molecular masses of 43, 31, 23 and 14 kDa. The three larger subunits are: cytochrome *b*, having two *b*-type hemes (b_{562} and b_{566}), cytochrome c_1, containing one *c*-type heme (c_1) and the iron–sulfur protein (ISP), including a [2Fe–2S] cluster [1,3]. These three subunits are present in all the cytochrome bc_1 complexes and are thus termed the core subunits. The smallest subunit contains no redox prosthetic group and is a supernumerary subunit [4,5]. While the study of the core subunits has been intensive and has produced a wealth of information, the study of supernumerary subunits has been rather limited. The presence of only one supernumerary subunit (subunit IV) in the *R. sphaeroides* complex provides us with an ideal system for the structural and functional study of the supernumerary subunit.

The gene for subunit IV (*fbc*Q) of *R. sphaeroides* bc_1 complex has been cloned and sequenced [6]. A mutant that lacks subunit IV (RSΔIV) has been constructed [7]. The cytochrome bc_1 complex purified from RSΔIV chromatophores contains only the three core subunits and has only a fraction of the wild-type complex activity [7]. Subunit IV has been over-expressed in *Escherichia coli* cells as a GST fusion protein and purified to homogeneity with a procedure involving glutathione agarose gel, thrombin digestion, and gel filtration [8]. When purified recombinant subunit IV was added to the three-subunit core complex, the bc_1 activity was restored to the level of the wild-type complex, indicating that recombinant subunit IV can properly assemble into the cytochrome bc_1 complex [8]. The availability of reconstitutively active, three-subunit core complex and recombinant subunit IV enables us to use an *in vitro* reconstitution approach to identify the amino acid residues of subunit IV involved in interaction with the core complex [9,10]. Residues 81–84, with a sequence of YRYR [10], and residues 86–109, which comprise the only transmembrane helix in subunit IV [9], are essential. It has been suggested that subunit IV is incorporated into the bc_1 complex through its transmembrane helix and then interacts with the core subunits through residues 81–84 to restore the bc_1 activity to the level of the wild-type complex [10]. However, it is not known how this interaction can restore the bc_1 activity.

Recently, we have observed several interesting results [11], including (i) in the three-subunit core complex, the extent of cytochrome *b* reduction by ubiquinol in the presence of antimycin A cannot reach the same level as that in the wild-type complex; (ii) the core complex produces 4 times more superoxide than the wild-type complex; and (iii) the activity of reconstituted complexes,

Abbreviations: ISP, iron–sulfur protein; $Q_0C_{10}BrH_2$, 2,3-dimethoxy-5- methyl-6-(10-bromodecyl)-1,4-benzoquinol; DM, dodecylmaltoside; OG, n-*octyl*-beta-D-glucopyranoside; $QoC10BrH_2$, 2,3-dimethoxy-5-methyl-(10-bromodecyl)1,4-benzoquinol; MCLA, 2-methyl-6-(4-methoxyphenyl)-3,7-dihydroimidazo[1,2-α]pyrazin-3-one hydrocholoride

* Corresponding author. Tel.: +1 405 744 6196; fax: +1 405 744 7799.
E-mail address: linda.yu@okstate.edu (L. Yu).

0005-2728/$ – see front matter © 2011 Elsevier B.V. All rights reserved.
doi:10.1016/j.bbabio.2011.10.005

formed from the core complex and subunit IVs, is inversely proportional to its superoxide production activity. Although these findings may suggest that subunit IV increases the bc_1 complex activity [11] by preventing electron leakage from the low potential electron transfer chain and thereby keeping electrons from reacting with molecular oxygen to produce superoxide anions [12–15], the mechanism through which subunit IV performs these functions is yet to be elucidated.

Apparently, crystallization of *R. sphaeroides* cytochrome bc_1 complex and subsequent three-dimensional structure analysis of this complex will provide invaluable information to our understanding of the function of subunit IV in the cytochrome bc_1 complex. Unfortunately, crystallization of the *R. sphaeroides* wild-type, four-subunit complex resulted in crystals containing only the three core subunits [16]. Apparently subunit IV was dissociated from the core complex during crystallization. Although crystals of this three-subunit core complex diffracted X-rays to 2.1 Å resolution [16], the lack of subunit IV limited the utility of this bacterial structure. One way to obtain a 3-D structure of the four-subunit complex is to covalently link subunit IV to one of the core subunits, thereby preventing the dissociation of subunit IV from the complex during crystallization. This approach is feasible only if the generated fusion mutant complex has similar or even better characteristics as compared to that of the wild type, four-subunit complex.

Here, we report procedures for generating *R. sphaeroides* mutants expressing His_6-tagged bc_1 complex with the N-terminus of subunit IV fused to the C-terminus of cytochrome c_1. Photosynthetic growth behavior, enzymatic activity, structural stability, and superoxide production of fusion mutant complexes with a polyglycine linker of two different lengths were examined and compared with the wild-type complex. Crystals of one such fusion mutant have also been obtained, diffracting X-rays to 5.5 Å resolution.

2. Materials and methods

Cytochrome *c*, (horse heart, type III), Ni-NTA gel, and QiAprep Spin Miniprep Kit were purchased from Sigma. N-dodecyl-ß-D-Maltopyranoside (DM) and N-octyl-ß-D-Glucopyranoside (OG) were purchased from Anatrace. Stigmatellin was purchased from Fluka. 2-Methyl-6-(4-methoxyphenyl)-3,7-dihydroimidazo[1,2-α]pyrazin-3-one, hydrochloride (MCLA) was purchased from Molecular Probes, Inc. 2,3-Dimethoxy-5-methyl-6-(10-bromodecyl)-1,4-benzoquinol ($Q_0C_{10}BrH_2$) was prepared in our laboratory as previously reported [17]. All other chemicals were of the highest purity commercially available.

2.1. Growth of bacteria

E. coli cells were grown at 37 °C in LB medium. An enriched Sistrom medium containing 5 mM glutamate and 0.2% casamino acids was used for photosynthetic growth of the plasmid-bearing *R. sphaeroides* cells [18]. The conditions for photosynthetic growth were similar to what has been described previously [19]. Antibiotics were added to growth media at the following concentrations: tetracycline, 10–15 mg/L, and trimethoprim, 25 mg/L for *E. coli*; tetracycline, 1 mg/L, kanamycin sulfate, 20 mg/L, and trimethoprim, 25 mg/L for *R. sphaeroides*.

2.2. Generation of R. sphaeroides mutants expressing His-tagged bc_1 complex with the N-terminus of subunit IV fused to the C-terminus of cytochrome c_1

Two mutants with the N-terminus of subunit IV fused to the C-terminus of cytochrome c_1 were constructed: one with a 6-glycine linker placed between the two fusing subunits and a 6-His tag at the C-terminus of subunit IV (c_1-6Gly-IV-6His); the other with a 14-glycine linker between the two fusing subunits and a 6-His tag at the C-terminus of subunit IV (c_1-14Gly-IV-6His). Scheme 1 outlines the strategy used for construction of c_1-6Gly-IV-6His. The construction was divided into three parts. The aim of part I was to generate an *Xba*I–*Xho*I DNA fragment encoding c_1-6Gly-IV-6His. This was achieved by three PCR amplification reactions: the first one was to generate a DNA fragment encoding c_1-6Gly (fragment A); the second one was to produce a DNA fragment encoding 6Gly-IV-6His (fragment B) and the third one was to generate a DNA fragment encoding c_1-6Gly-IV-6His (fragment C). The first two PCR reactions used the pRKD*fbcFBC*$_{6H}$*Q*[19] as template, and the third PCR amplification reaction used a mixture of fragments A and B as templates. The forward and reverse primers used (see Table 1) were: c_1-6Gly(F) and c_1-6Gly(R) for the first PCR amplification; 6Gly-IV-6His (F) and 6Gly-IV-6His(R) for the second; and c_1-6Gly(F) and 6Gly-IV-6His(R) for the third. The produced DNA fragment C was digested with *Xba*I and *Xho*I to generate an *Xba*I–*Xho*I fragment encoding c_1-6Gly-IV-6His. The goal of part II was to ligate the *Xba*I–*Xho*I fragment into the *Xba*I and *Xho*I digested pRKD*fbcFBC*$_{6H}$*Q* plasmid and then transform the resulting plasmid, pRKD*fbcFBC*$_{6G}$*Q*$_{6H}$, into *E. coli* S17 cells. In part III, we transferred pRKD*fbcFBC*$_{6G}$*Q*$_{6H}$ from *E. coli* S17 cells to *R. sphaeroides* BC17 cells by plate conjugation according to previously reported procedures [18–20].

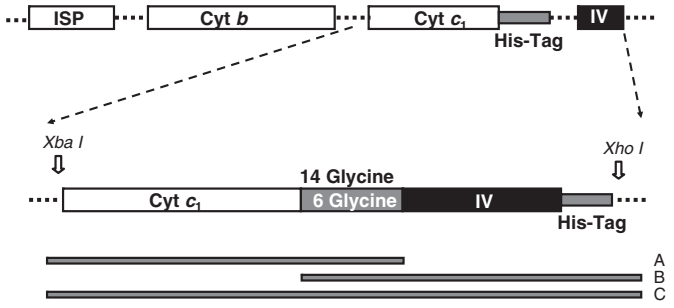

Scheme 1. Strategy for the construction of the c_1-6Gly-IV-6His mutant.

The c_1-14Gly-IV-6His mutant was constructed by the same protocol used for construction of mutant c_1-6Gly-IV-6His except that the reverse primer used in generation of fragment A was c_1-10Gly(R) and the forward primer for fragment B was 10Gly-IV-6His (F) (see Table 1). It should be noted that when the generated fragments A and B (each encoding 10 glycines) were used as templates for generating fragment C at the annealing temperature of 56 °C, only DNA encoding 6 glycines from each fragment was paired, resulting in 14 glycines between cytochrome c_1 and subunit IV.

2.3. Purification of mutant complexes and the activity assay

Chromatophore membranes were prepared from wild-type and mutant cells. The cytochrome bc_1 complexes were purified from chromatophores as described previously [20] and stored at −80 °C containing 10% glycerol until use. The concentrations of cytochromes *b*

Table 1
The oligonucleotides used for mutations.

c_1-6Gly(F)	5′ CTAG TCT AGA AGG GAA AGG ACA GTG 3′
c_1-6Gly(R)	5′ GCC ACC GCC ACC GCC ACC GAC GTT CGT CTT CTT CTT GCC 3′
6Gly-IV-6His(F)	5′ GGT GGC GGT GGC GGT GGC ATG TTC TCA TTC ATC GAC GAC3′
6Gly-IV-6His(R)	5′ CCG CTC GAG TTA GTG ATG GTG GTG GTG ATG TTC GAT GGG ATA GAC GAC GCT 3′
c_1-10Gly(R)	5′ GCC ACC GCC ACC GCC ACC GCC ACC GCC ACC GAC GTT CGT CTT CTT CTT GCC 3′
10Gly-IV-6His (F)	5′ GGT GGC GGT GGC GGT GGC GGT GGC GGT GGC ATG TTC TCA TTC ATC GAC GAC 3′

[21] and c_1 were determined spectrophotometrically and calculated using published molar extinction coefficients.

To assay the activity of ubiquinol–cytochrome *c* reductase, chromatophores or purified cytochrome bc_1 complexes were diluted with 50 mM Tris–HCl buffer, pH 8.0, containing 200 mM NaCl and 0.01% DM to a final concentration of cytochrome *b* of 1 μM. Appropriate amounts of the diluted proteins were added to 1 mL of assay mixture containing 100 mM Na^+/K^+ phosphate buffer, pH 7.4, 1 mM EDTA, 50 μM cytochrome *c*, and 25 μM $Q_0C_{10}BrH_2$. The reduction of cytochrome *c* was measured by the increase of the absorbance at 550 nm wavelength in a Shimadzu UV-2401 PC spectrophotometer at 23 °C. A millimolar extinction coefficient of 18.5 [22] was used for calculation of the activity. The non-enzymatic oxidation of $Q_0C_{10}BrH_2$, before the addition of enzyme, was subtracted in the calculation of specific activity. $Q_0C_{10}BrH_2$ is a better substrate than $Q_0C_{10}H_2$ for the cytochrome bc_1 complex [17].

2.4. Gel electrophoresis and Western blot

The SDS-PAGE was performed with a Bio-Rad Mini-Protein dual slab vertical cell. Samples were treated with a sample buffer containing 10 mM Tris–HCl buffer, pH 6.8, 1% SDS, 3% glycerol and 0.4% β-mercaptoethanol (β-ME) for 10 min at room temperature before electrophoresis. The polypeptides on SDS-PAGE gel were transferred to 45 μm nitrocellulose membrane and probed with antibodies against subunit IV or against cytochrome c_1 of the *R. sphaeroides* bc_1 complex. Horseradish peroxidase (HRP) conjugated protein A was used as secondary antibody. HRP color development solution (Bio-Rad) was used to detect the protein bands that specifically reacted to the antibodies.

2.5. Enzyme-linked immunosorbent assay (ELISA)

A modified ELISA [23] was used for quantitative comparison of subunit IV in the wild-type and c_1-14Gly-IV-6His mutant complexes. The wild-type and mutant complexes were diluted with a carbonate buffer, pH 9.5, containing 15 mM Na_2CO_3, 35 mM $NaHCO_3$, and 0.02% NaN_3, to a protein concentration of 10 μg/mL. Aliquots of 100 μL of diluted enzyme solutions were added to each well of the ELISA plate and incubated, overnight, at 4 °C. After incubation, the unbound bc_1 complex was removed from the well and blocking buffer (1% casein in PBS buffer containing 137 mM NaCl, 2.7 mM KCl, 8.1 mM $Na_2HPO_4{\bullet}2H_2O$, and 1.76 mM KH_2PO_4, pH 7.4) was added. After the plate was incubated at 37 °C for 1 h, the blocking buffer was then removed and the wells were washed with 280 μL of PBS buffer. An aliquot of 125 μL of 1:500 diluted anti-subunit IV antibody was added per well and the plate was incubated at room temperature for 1 h. The wells were then washed 3 times with PBS buffer. The horseradish peroxidase (HRP)-conjugated Protein A was added as the second antibody and incubated for another hour. After washing, binding of the second antibody was detected by applying 100 μL of tetramethyl benzidine (TMB) substrate. The reaction was stopped by adding 100 μL of 1 N HCl to each well. The plate was read at 450 nm using a multi-well plate reader.

2.6. Differential scanning calorimetry (DSC) measurement

DSC measurements were performed using Nano-DSC II from Calorimetry Sciences Corp. The sample and reference solutions were degassed before use. The wild-type and c_1-14Gly-IV-6His mutant complexes were diluted with a degassed buffer containing 100 mM Na^+/K^+ phosphate, pH 7.4, and 0.01% DM to a final concentration of 2 mg/mL(36 μM of cytochrome b). The diluted protein solution was then injected into the sample cell and the control buffer into the reference cell. The data acquisition DSC program (10–90 °C/3 scans) was run at a rate of 1 °C/min. The cells were equilibrated for 10 min before the heating and cooling processes. The DscRun program recorded the input heat flow difference between the sample cell and reference cell and plotted the data as a function of temperature. The CpCalc program calculated transition temperature and enthalpy change of transition using the second heating as a baseline for analysis.

2.7. Quantitative comparisons of the iron–sulfur cluster in the wild-type and fused mutant complexes by EPR

Aliquots of 300 μL of purified wild-type and mutant cytochrome bc_1 complexes (cytochrome $b = 100$ μM) were treated with 5-fold excess of ascorbate to fully reduce cytochrome c_1 and frozen in liquid nitrogen. EPR spectra were recorded at −150 °C in a Bruker EMX EPR spectrometer with the following instrument settings: center field, 3600 G; microwave frequency, 9.397021 GHz; microwave power 2.16 mW; modulation frequency, 100.00 kHz; modulation amplitude, 6.3 G; time constant, 655.36 ms; conversion time, 163.84 ms; sweep time, 167.77 s; number of X-scans, 4.

2.8. Determination of superoxide production

The production of superoxide anion by the cytochrome bc_1 complex was determined by measuring the chemiluminescence of the MCLA-O_2^- adduct [24] in an Applied Photophysics Stopped-flow Reaction Analyzer SX.18 MV (Leatherhead, England), while leaving the excitation light off and registering light emission [25,26]. Reactions were carried out at 23 °C by mixing solutions I and II in a 1:1 ratio. Solution I contained 100 mM Na^+/K^+ phosphate buffer, pH 7.4, 1 mM EDTA, 1 mM KCN/ 1 mM NaN_3, 0.1% bovine serum albumin, 0.01% DM, and wild-type or mutant bc_1 complex (4 μM cytochrome *b*). Solution II contained 100 mM Na^+/K^+ phosphate buffer, pH 7.4, 1 mM EDTA, 1 mM KCN/1 mM NaN_3, 0.1% bovine serum albumin, 0.01% DM, 67 μM $Q_0C_{10}BrH_2$ and 4 μM MCLA.

2.9. Protein crystallization

The purified c_1-14Gly-IV-6His mutant complex was diluted to a protein concentration of 12 mg/mL with a buffer containing 50 mM Tris–HCl, pH 7.5, 200 mM NaCl, 10% glycerol, 5 mM NaN_3, 0.5% β-OG (Anatrace) and 200 mM histidine. The diluted protein solution was treated with a 5-fold molar excess of stigmatellin at 4 °C for 5 h. An aliquot of the solution was augmented with 0.06% sucrose monocaprate (Fluka), 50 mM potassium nitrate, and 8% PEG 400. The solution was incubated overnight at 4 °C and centrifuged at 44,000×*g* to remove precipitates, if any. The supernatant was used in sitting drop crystallization experiments at 15 °C. The reservoir solution contained 100 mM Tris-Cl, pH 8.0, 600 mM NaCl, 20% glycerol, 5 mM NaN_3, and 26% PEG 400.

3. Results and discussion

3.1. The rationale for the generation of mutants expressing cytochrome bc_1 complex with the N-terminus of subunit IV fused to the C-terminus of cytochrome c_1

One approach used to prevent subunit IV from dissociating from the three-subunit core complex during crystallization is to generate mutants with subunit IV fused into one of the three core subunits (cytochrome *b*, cytochrome c_1 or ISP) of the cytochrome bc_1 complex. Two fusion mutants, c_1-6Gly-IV-6His and c_1-14Gly-IV-6His, in which the N-terminus of subunit IV is fused to the C-terminus of cytochrome c_1, with a 6- or 14-glycine linker between the two fusing subunits and a 6-his tag at the C-terminus of subunit IV, were constructed for this study.

The decision to fuse the N-terminus of subunit IV to the C-terminus of cytochrome c_1 is based on the following information:

(i) the structural model of subunit IV indicates a single transmembrane helix in the subunit; (ii) the study of the topological arrangement of subunit IV in the chromatophore membrane [9] indicates that the N-terminus of the subunit is located at the cytoplasmic side of the membrane; (iii) the 3-D structural information of the *R. sphaeroides* three-subunit core complex 2QJY [16] shows that the C-terminus of cytochrome c_1 subunit is on the cytoplasmic side.

The current structural model of subunit IV in the c_1-14Gly-IV-6His mutant complex, as shown in Fig. 1 with the red color, was constructed by the following ways: (i). The TMHMM and TMpred programs [27,28] predict a single transmembrane helix for subunit IV with nearly 100% probability from residues 87 to 105. (ii). The predicted helix was aligned with subunit VII from bovine heart mitochondrial bc_1. Despite the low sequence identity, the C-terminal ends of subunit IV and beef VII show a sequence pattern that allows a plausible alignment. (iii). The transmembrane helix of beef subunit VII is preceded by a horizontally extended helix featuring a number of polar residues. Similar to that, the putative TM helix of subunit IV is preceded by a polar helix (by secondary structure prediction) of comparable length. (iv). Subunit VII of beef mitochondrial bc_1 was used as a template for subunit IV from residues 64 to 104. (v). Residues 1–63 were modeled by I-Tasser [29] producing only domains with low scores due to the as of yet unique sequence of subunit IV. The best of the five models that I-Tasser produced was combined with the segment that was modeled using beef subunit VII as template. (vi). It is directly connected residue 1 of the modeled subunit IV with a 14-Gly linker (shown in magenta color) to the C-terminus of cytochrome c_1. A 14-Gly linker in the fully extended (beta-strand) form covers a distance of 14×3.32 Å $= 46.5$ Å, and the N-terminal end of sub IV is well within the reach of this linker. (vii). The model was then energy minimized and arranged in a way that is compatible (no clashes) with the current crystallographic data (cell dimensions and space group).

The topological arrangement of the transmembrane helix in the proposed structural model of subunit IV was determined previously using antibodies against synthetic peptides corresponding to the near N-terminal and the C-terminal peptides, in sealed (inside-out) and broken chromatophores [9]. Since antibodies against the C-terminal peptide react only with the broken chromatophores while antibodies against N-terminal peptide react with both sealed and broken chromatophores, the N-terminal end of subunit IV is exposed on the cytoplasmic side and the C-terminal end is on the periplasmic side of the chromatophore membrane. This topological arrangement study placed the first 85 amino acid residues of subunit IV on the cytoplasmic side of the membrane, where more space is available for proper folding of this large portion of subunit. Since the N-terminus of subunit IV is located on the cytoplasmic side of the membrane, the need for the generation of fusion mutants with the N-terminus of subunit IV on the periplasmic side of the chromatophore membrane is eliminated.

In the recently available 3-D structure of the *R. sphaeroides* three-subunit core complex [16], the C-terminus of cytochrome c_1, and the N- and C-terminus of cytochrome *b* are located on the cytoplasmic side of the membrane. Therefore, by fusing the N-terminus of subunit IV into the C-termini of either cytochrome c_1 or cytochrome *b* (see Fig. 1), one should obtain a mutant bc_1 complex with correct orientation of subunit IV, i.e., the N-terminus is located on the cytoplasmic side of the membrane. Although the cytochrome *b* subunit also has its C-terminus at the cytoplasmic side, we decided to fuse the subunit IV gene to the cytochrome c_1 gene instead of the cytochrome *b* gene, because the cytochrome *b* subunit is located at the innermost section of the complex. It is very likely that a fusion of subunit IV with the C-terminus of cytochrome *b* would prevent proper assembly, leading to interferences in the interactions between cytochromes *b* and c_1 and/or ISP.

In order to increase the structural flexibility of the fused subunits, a linker of 6 or 14 glycine residues was introduced between the two fusing subunits. Glycine was chosen as the linker residue because it is the smallest amino acid with the greatest flexibility. Introducing the glycine linker should preserve the structural integrity of the two fused subunits in the bc_1 complex. The length of glycine linker selected was somewhat arbitrary. Although a 14-glycine linker is calculated to be sufficient to cover the distance from the C-terminus of cytochrome c_1 to the N-terminus of subunit IV, it is still possible that a linker longer than 14 glycine is needed. We chose a 6- and 14-glycine linker to start this study and with intention to use a longer glycine linker if these two linkers are proved experimentally not to be long enough. To facilitate the purification of mutant complexes, a 6-histidine tag was introduced at the C-terminus of subunit IV.

3.2. Photosynthetic growth behavior of c_1-6Gly-IV-6His and c_1-14Gly-IV-6His mutants

Because a functional bc_1 complex is absolutely required for the photosynthetic growth of *R. sphaeroides*, the degree to which these two fusion constructs affect the activity of the complex can be determined by analyzing their photosynthetic growth behavior. Wild-type and mutant cells harboring c_1-6Gly-IV-6His or c_1-14Gly-IV-6His bc_1 complexes grown aerobically in mid-log phase were transferred into Sistrom medium at the same cell density and subjected to anaerobic photosynthetic growth conditions (see Fig. 2). The wild-type cells began exponential growth after a lag phase of 24 h, whereas

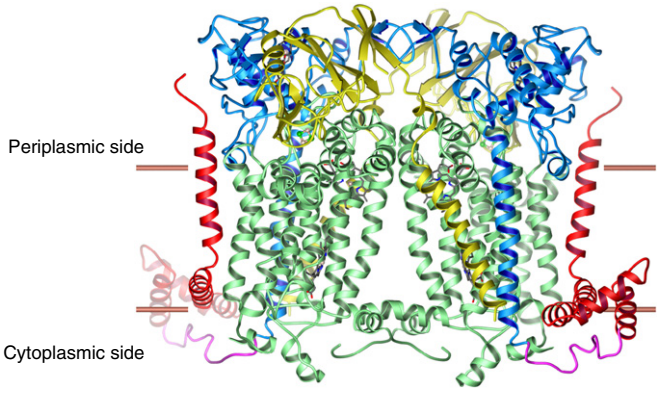

Fig. 1. Structural model of subunit IV in the c_1-14Gly-IV-6His mutant complex. Subunit IV is in red, cyt. *b* in light green, ISP in yellow and cyt. c_1 in royal blue. The 14-glycine linker is in magenta.

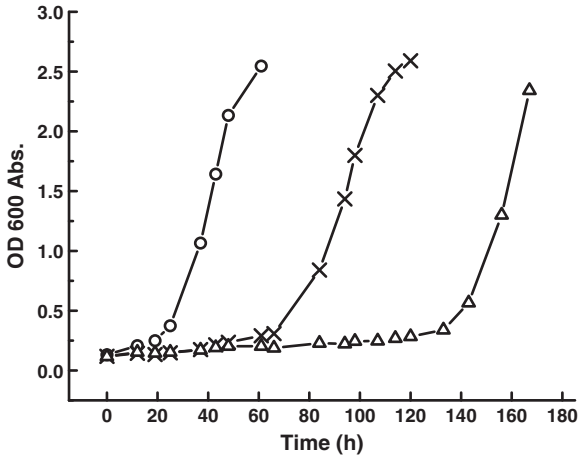

Fig. 2. Photosynthetic growth of *R. sphaeroides* strains. Aliquots of mid-log phase aerobically grown wild type (o), c_1-14Gly-IV-6His (x) and c_1-6Gly-IV-6His (Δ) cells were inoculated into Sistrom A minimal medium containing 20 μg/mL kanamycin, 25 μg/mL trimethoprim, and 1 μg/mL tetracycline. Growth was monitored at $OD_{600\ nm}$.

c_1-14Gly-IV-6His and c_1-6Gly-IV-6His mutant cells began growth after a lag of 64 and 120 h, respectively. This indicates that fusion constructs caused the delay of photosynthetic growth. The length of delay for photosynthetic growth increased as the length of glycine linker in the fusion mutant decreased, suggesting that the lag time for photosynthetic growth decreased as the structural flexibility between the N-terminus of subunit IV and the C-terminus of cytochrome c_1 increased. The delay of photosynthetic growth is also observed for *R. sphaeroides* mutants lacking subunit IV [9] and for alanine substitution at residues 100–103 of ISP [30].

It is rather surprising that after such a long lag time, these two fusion mutants started to grow photosynthetically at a rate comparable to that of the wild-type cells. Although, at present, we do not know how the seemingly photosynthetically incompetent mutant strains develop into photosynthetically competent phenotype, we do incline to believe that this event is a consequence of adaptation rather than mutation in the *bc* operon or elsewhere in the genome. Adaptation was supported by re-growing the photosynthetically grown wild-type and mutants c_1-14Gly-IV-6His and c_1-6Gly-IV-6His cells under aerobic conditions and observing a lag of 24, 64 and 120 h in their respective growth curves, when these cells were again grown under photosynthetic conditions. If this event was a consequence of reverse mutation somewhere in the genome of *R. sphaeroides*, one would expect that this mutation is heritable and the resulting mutant when re-grew under photosynthetic conditions should behave like the wild-type with a lag of 24 h. Adaptation was further substantiated by finding the mutation-free *fbcF,B,C,Q* genes isolated from photosynthetically grown mutants c_1-6Gly-IV-6His and c_1-14Gly-IV-6His. Also, Western blotting analysis using anti-subunit IV and anti-c_1 antibodies detected no free c_1 and subunit IV in chromatophore and purified complexes isolated from the fused mutants.

One potential reason for the need of such long lag phase for the fused mutants to start photosynthetic growth is to change the membrane structure (or to modify the lipid environment of the mutant complex) to allow electrons to be transferred from the reaction center to the fused mutant complex. When adapted photosynthetically grown mutants re-grew under aerobic conditions, the membrane structures (or lipid environments) were reverted back to the original one and thus the mutants needed a long lag phase again to start photosynthetic growth. Since the c_1-6Gly-IV-6His mutant complex is structurally less flexible than the c_1-14Gly-IV-6His mutant complex, at least at the fused region, therefore it needs a longer lag phase to change the membrane structure (or lipid environment) than that of mutant c_1-14Gly-IV-6His.

3.3. Characterization of the c_1-14Gly-IV-6His mutant complex

When chromatophores were prepared from adapted, photosynthetically grown mutants c_1-6Gly-IV-6His or c_1-14Gly-IV-6His, the specific cytochrome *b* contents in these two mutant chromatophores were comparable to that in the wild-type chromatophore (0.8 ± 0.1 nmol cytochrome *b*/mg protein). Purification of mutant bc_1 complexes using DM solubilization followed by Ni-NTA affinity gel chromatography under the same conditions, however, generated different results. The yield of purified c_1-14Gly-IV-6His mutant was comparable to that of wild-type (12%), whereas the yield of purified c_1-6Gly-IV-6His mutant complex was extremely low (<1%). The yield was defined as % of the total cytochrome bc_1 complex (based on cytochrome *b* or cytochrome c_1 content) present in a given volume of chromatophore recovered in the final purified state. Since only very little of bc_1 complex from c_1-6Gly-IV-6His mutant was able to bind to the Ni-NTA column, the structures of cytochrome c_1 and subunit IV in this fused mutant complex may have been altered to the point that the His-tag became less accessible. Therefore, this mutant was eliminated from this study.

The absorption spectra of cytochromes *b* and c_1 in purified c_1-14Gly-IV-6His mutant complex (see Fig. 3B) were similar to those in the wild-type complex (see Fig. 3A). The cytochrome *b* content in the mutant complex (9.6 ± 0.1 nmol/mg protein) was also comparable to that in the wild-type complex (10.0 ± 0.1 nmol/mg protein). The ratio between cytochrome *b* and cytochrome c_1 in this mutant complex was around 1.4 (see Fig. 3, A and B), similar to that in the wild-type complex. The iron–sulfur cluster contents in purified wild-type and c_1-14Gly-IV-6His mutant complexes were comparable, judging by the EPR signal at $g_y = 1.89$ (see Fig. 3C).

Fig. 4A shows SDS-PAGE of the purified wild-type and c_1-14Gly-IV-6His mutant complexes. As expected, the wild-type complex shows four major protein bands with apparent molecular masses of 43, 31, 23, and 14 kDa (see lane 2 of Fig. 4A) corresponding to cytochrome *b*, cytochrome c_1, Rieske iron–sulfur protein, and subunit IV. The purified mutant complex, on the other hand, shows only three major protein bands with apparent molecular masses of 46, 43 and 23 kDa, respectively (see lane 3 of Fig. 4A). Although the separation between the two large proteins was not optimum due to their close molecular weight, it is expected that the 43-kDa protein band is cytochrome *b* while the 46 kDa band is the fused adduct of cytochrome c_1 and subunit IV.

To further confirm that the 46 kDa protein band observed in the mutant complex is a c_1–IV fusion protein, both the wild-type and mutant complexes were subjected to Western blot analysis using antibodies against *R. sphaeroides* cytochrome c_1 (Fig. 4B) and antibodies against *R. sphaeroides* subunit IV (Fig. 4C). In the wild-type complex, antibodies against cytochrome c_1 and subunit IV detected the cytochrome c_1 protein (Mw = 31 kDa) and subunit IV protein (Mw = 14 kDa) respectively. In the mutant complex, however, only a single band at a molecular weight of 46 kDa was recognized. This result confirmed that in the c_1-14Gly-IV-6His mutant complex subunit IV and cytochrome c_1 are fused together as a protein with an apparent molecular weight of 46 kDa.

When purified c_1-14Gly-IV-6His mutant complex was subjected to ubiquinol–cytochrome *c* reductase activity assay, it showed a specific activity of 4.0 ± 0.2 μmol cyt. *c* reduced per min per nmol cyt. *b*, which is 60% higher than that of the wild-type complex (2.5 ± 0.1 μmol cyt. *c* reduced per min per nmol cyt. *b*). As the observed higher activity for the mutant complex was a surprise, extra care was taken in purification steps. Specifically, we have carried out the purification experiments of wild-type and mutant proteins, side by side using the same detergent and buffers, multiple times. For each batch of the preparations, the activity was determined with the same assay mixture and substrate five times, reducing the error in the average specific activity to 5%. The increased activity observed in the c_1-14Gly-IV-6His mutant complex is most likely due to the presence of more subunit IV in the mutant complex than that in the wild-type complex. In the c_1-14Gly-IV-6His mutant complex, subunit IV is fused to cytochrome c_1 and a 6-His tag is placed at the C-terminal end of subunit IV, therefore no loss of subunit IV should occur during the purification process. Thus, a unit ratio between subunit IV and cytochrome c_1 should be present in the purified mutant complex. In the wild-type complex, a 6-His tag is placed at the C-terminal end of the cytochrome c_1 subunit, and the amount of subunit IV associated with cytochrome c_1 depends on the binding affinity of subunit IV to cytochrome c_1 under the detergent concentration used during purification process. Some loss of subunit IV is expected. In this case, a less than unit ratio between subunit IV and cytochrome c_1 would be present in the wild-type complex.

As predicted, when the wild-type and mutant complexes were subjected to an ELISA assay using antibodies against subunit IV, the mutant complex had about 30 ± 3% more subunit IV than the wild-type complex. It should be noted that the absolute amounts of subunit IV in the wild-type and mutant complexes cannot be accurately determined based on the color intensities of antibody reacting to subunit IV bands in Western blot simply because the blotting efficiencies

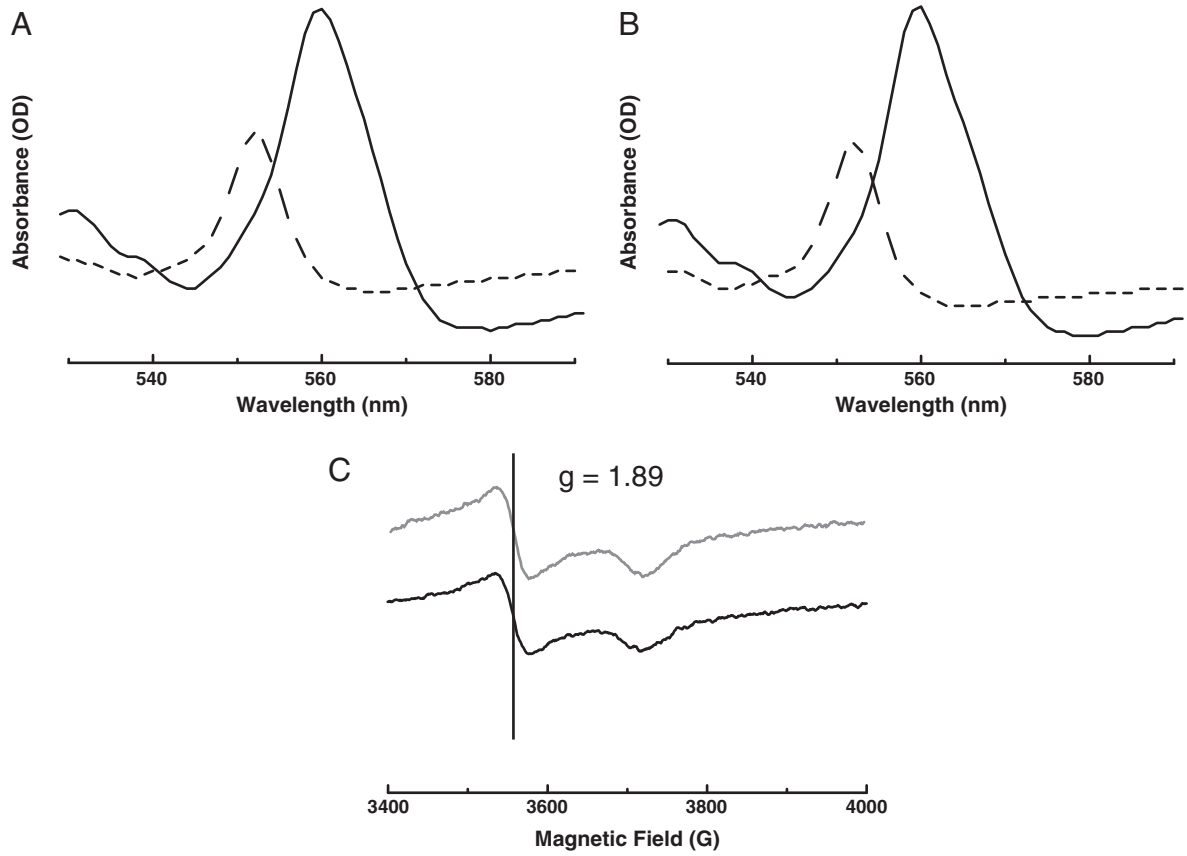

Fig. 3. The absorption and EPR spectra of cytochromes *b* and c_1 in the wild type and c_1-14Gly-IV-6His mutant complexes. The difference absorption spectra of cytochrome *b* (solid lines) and cytochrome c_1 (dashed lines) in the wild-type (A) and c_1-14Gly-IV-6His (B) mutant complexes. The difference spectra of cytochrome *b* were determined by measuring the dithionite reduced minus the ascorbate reduced samples and the difference absorption spectra of cytochrome c_1 were determined by measuring the ascorbate reduced minus the ferricyanide oxidized samples. C. EPR spectra of the wild-type (black line) and c_1-14Gly-IV-6His (gray line) mutant complexes. The experimental conditions were as described in Section 2.

of the free and the c_1–IV fused subunit IV may be different due to the difference in their molecular masses.

In order to ascertain that the activity increase observed in the c_1-14Gly-IV-6His mutant complex is indeed due to the presence of more subunit IV in the mutant complex, purified recombinant subunit IV was added to the wild-type complex and electron transfer activity was assayed. Maximum activity of 4.3 ± 0.2 μmol *c* reduced per min per nmol *b* was obtained when a molar excess of subunit IV was added, indicating that this wild-type complex preparation was somewhat deficient in subunit IV. However, we cannot use this result as a basis to conclude that all the previously prepared wild-type complexes with reported specific activities of less than 4.3 ± 0.2 μmol *c* reduced per min per nmol *b* were deficient in subunit IV. This is because the activity of this bacterial complex varies greatly by the detergent (type and concentration) used in solubilization, purification and assay, and the ubiquinol derivative ($Q_0C_{10}BrH_2$, $Q_0C_{10}H_2$, or Q_2H_2) used as substrate. The only way to determine whether or not a preparation of the wild-type complex is deficient in subunit IV is to add subunit IV to the prepared complex and assay the activities of the wild-type complex alone and subunit IV added wild-type complex at the same time under identical conditions. An increase in activity indicates a deficiency of subunit IV in the complex, no change in activity indicates no deficiency of subunit IV in the complex.

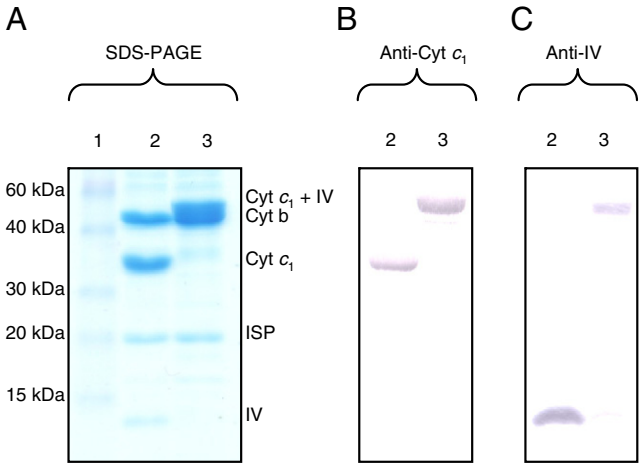

Fig. 4. SDS-PAGE and Western blot analyses of purified wild type and c_1-14Gly-IV-6His mutant complexes. A. SDS-PAGE pattern. Lanes 1–3 were protein standards, wild-type and mutant complexes, respectively. B. Western blot using antibody against *R. sphaeroides* cytochrome c_1 as the primary antibody. Lanes 2 and 3 were the wild-type and mutant complexes, respectively. C. Western blot using antibody against *R. sphaeroides* subunit IV as the primary antibody. Lanes 2 and 3 were the wild-type and mutant complexes, respectively.

Fig. 5 compares the superoxide production by the wild-type and mutant c_1-14Gly-IV-6His complexes measured with the chemiluminescence method [25,26]. The MCLA-$O_2^{\cdot-}$ chemiluminescence induced by the wild type bc_1 complex reached its maximum peak height (0.17 V) and then decreased. A maximum peak intensity of 0.11 V was induced by the c_1-14Gly-IV-6His mutant complex, which was about 30% less than that of the wild-type complex. The observation that the c_1-14Gly-IV-6His mutant complex has a higher electron transfer activity but a lower superoxide producing activity as compared to the wild-type complex is consistent with our previous

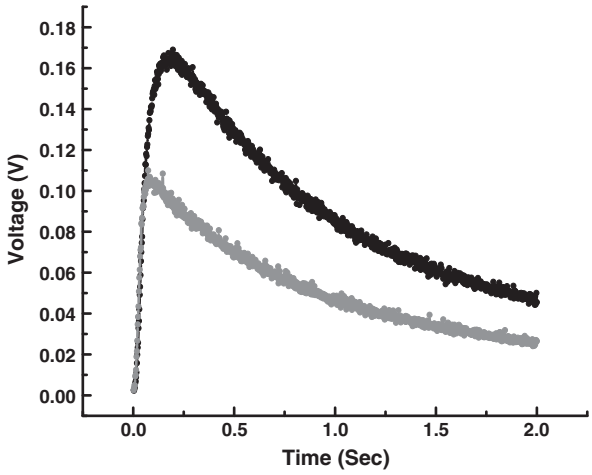

Fig. 5. Superoxide generation by the wild-type and c_1-14Gly-IV-6His mutant complexes. The experimental conditions were as described in Section 2. The produced chemiluminescence in voltage was monitored in 2 s. The black line represents the wild-type complex and the gray line represents the mutant complex.

finding [31] in which the electron transfer activity is inversely proportional to the superoxide-generating activity in the bc_1 complex.

The c_1-14Gly-IV-His mutant complex is structurally more stable than the wild-type enzyme, as shown by the fusion mutant complex's higher tolerance to detergent treatment and its higher thermotropic denaturation temperature as compared to the wild-type complex. As shown in Fig. 6, the treatment of purified wild-type and c_1-14Gly-IV-6His mutant complexes with varying concentrations of DM led to decreased activity with increasing concentrations of the detergent. However, the extent of activity decrease, at a given concentration of DM treatment, was less in the mutant complex than that in the wild-type complex. At 0.013% of DM (130 μg/mL) treatment, the wild-type protein (100 μg/mL) lost ~81% of its electron transfer activity, whereas the mutant protein (104 μg/mL) lost only ~36%, indicating that the c_1-14Gly-IV-6His mutant complex is structurally more stable than the wild-type protein. This was further verified by a DSC experiment where the thermotropic properties of the purified wild type and mutant proteins were analyzed and compared. Fig. 7 shows DSC thermograms of the wild-type and c_1-14Gly-IV-6His mutant complexes. When the wild type complex underwent thermodenaturation, it showed a *T*m of 45.3 °C and Δ*H* of 128.7 kcal/mol.

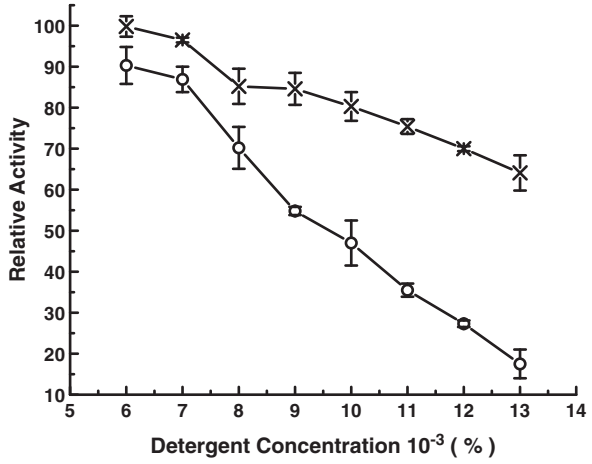

Fig. 6. Effect of DM concentration on the bc_1 activities of the wild-type and c_1-14Gly-IV-His mutant complexes. The wild-type (o) and mutant (x) complexes, 1 μM cytochrome *b*, were treated with indicated concentrations of DM and incubated for 1 h on ice. Aliquots were then withdrawn for bc_1 activity assays. The purities of wild type and mutant complexes used were 10.0 and 9.6 nmol cytochrome *b* per mg protein, respectively. The 100% activity was set as 4.86 μmol cyt.*c* reduced/min/nmol cyt.*b*.

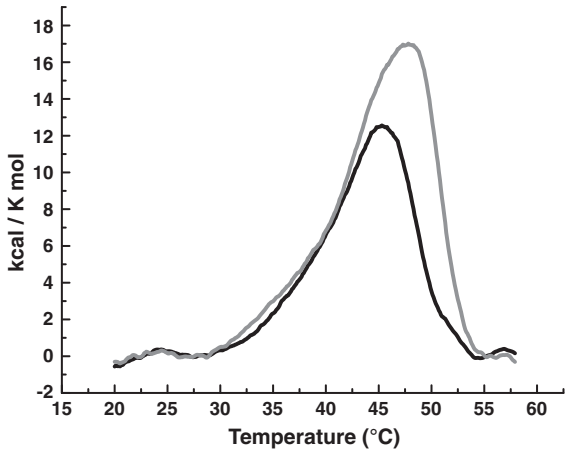

Fig. 7. Differential scanning calorimetry of the wild-type and c_1-14Gly-IV-His mutant complexes. The curve with black line represents the wild-type complex and the gray line represents the mutant complex.

Under the same conditions, the c_1-14Gly-IV-6His complex had a *T*m of 47.8 °C and Δ*H* of 187.7 kcal/mol. The increase in *T*m of the mutant complex indicates that this fusion mutant complex need higher temperature to unfold the protein and is thermodynamically more stable than the wild-type complex. Furthermore, when the complexes were kept at room temperature for 20 h, the wild-type complex lost about 42% of its electron transfer activity, whereas the mutant complex lost only about 14% of its activity (data not shown).

3.4. Crystallization and preliminary X-ray diffraction analysis

Crystals of the stigmatellin treated mutant c_1-14Gly-IV-6His complex (see Fig. 8) were obtained only when the Sr^{2+} ions which was added during crystallization of the wild-type complex was replaced with the K^+ ions (~50 mM). The mutant crystals contained four protein subunits as revealed by SDS-PAGE and Western blots. The crystals were flash frozen in liquid propane and maintained at a temperature of 100 K during X-ray data collections at the Advanced Photon Source (APS) at the Ser-CAT beamline 22. The diffraction pattern of the best crystal extended to 5.5 Å and displayed the symmetry of space group $P4_22_12$. We are in the process of optimizing crystallization conditions aiming at obtaining crystals of higher quality. It is expected that a higher resolution structure of the 4-subunit cytochrome bc_1 complex will be obtained when a better crystal preparation is achieved.

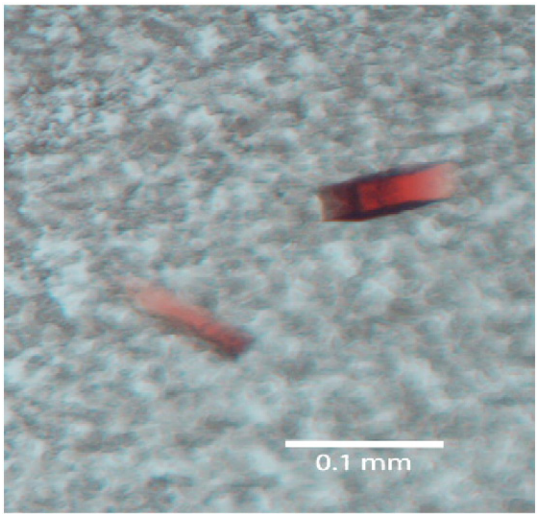

Fig. 8. Crystals of c_1-14Gly-IV-6His mutant complex.

4. Concluding remarks

The X-ray crystallography has emerged as a dominant technique for structure determination of membrane protein complexes. The loss of integral components or subunits during complex crystallization has been observed, leading to incomplete structural information and demanding remedies for improvement in complex preparation and crystallization procedure. In this work, we explore the genetic approach of covalently linking the interested subunit to other more stable subunits in a protein complex in order to mitigate the problem of subunit loss during crystallization. The data presented here confirms the usefulness of this approach using bacterial cytochrome bc_1 complex as a model system. The key points that this paper deals with are: (i) the loss of subunit IV in *R. sphaeroides* bc_1 complex during crystallization can be prevented by fusing the subunit IV gene with the gene of a core subunit, and the structural constraint thus introduced can be alleviated by placing a poly-glycine linker of proper length between these two fused subunits, (ii) the mutant strain typically require a longer than expected adaptation time, and (iii) the fusion protein displays better than expected properties, which are required for the structure-function study of the cytochrome bc_1 complex.

Acknowledgements

This work was supported in part by a grant from NIHGM030721 and the Oklahoma Agricultural Experiment Station Projects #1819 and #2372, and the Intramural Research Program of the NIH, National Cancer Institute.

References

[1] B.L. Trumpower, R.B. Gennis, Energy transduction by cytochrome complexes in mitochondrial and bacterial respiration: the enzymology of coupling electron transfer reactions to transmembrane proton translocation, Annu. Rev. Biochem. 63 (1994) 675–716.
[2] A.R. Crofts, The cytochrome bc_1 complex: function in the context of structure, Annu. Rev. Physiol. 66 (2004) 689–733.
[3] X.H. Yang, B.L. Trumpower, Protonmotive Q cycle pathway of electron transfer and energy transduction in the three-subunit ubiquinol–cytochrome *c* oxidoreductase complex of *Paracoccus denitrificans*, J. Biol. Chem. 263 (1988) 11962–11970.
[4] P.O. Ljungdahl, J.D. Pennoyer, D.E. Robertson, B.L. Trumpower, Purification of highly active cytochrome bc_1 complexes from phylogenetically diverse species by a single chromatographic procedure, Biochim. Biophys. Acta 891 (1987) 227–241.
[5] L. Yu, C.A. Yu, Essentiality of the molecular weight 15,000 protein (subunit IV) in the cytochrome b–c_1 complex of *Rhodobacter sphaeroides*, Biochemistry 30 (1991) 4934–4939.
[6] S. Usui, L. Yu, I.V. Subunit, (Mr = 14,384) of the cytochrome b–c_1 complex from *Rhodobacter sphaeroides*. Cloning, DNA sequencing, and ubiquinone binding domain, J. Biol. Chem. 266 (1991) 15644–15649.
[7] Y.R. Chen, S. Usui, C.A. Yu, L. Yu, Role of subunit IV in the cytochrome bc_1 complex from *Rhodobacter sphaeroides*, Biochemistry 33 (1994) 10207–10214.
[8] Y.R. Chen, C.A. Yu, L. Yu, Functional expression of subunit IV of *Rhodobacter sphaeroides* cytochrome b–c_1 complex and reconstitution of recombinant protein with three-subunit core complex, J. Biol. Chem. 271 (1996) 2057–2062.
[9] S.C. Tso, S.K. Shenoy, B.N. Quinn, L. Yu, Subunit IV of cytochrome bc_1 complex from *Rhodobacter sphaeroides*. Localization of regions essential for interaction with the three-subunit core complex, J. Biol. Chem. 275 (2000) 15287–15294.
[10] S.C. Tso, Y. Yin, C.A. Yu, L. Yu, Identification of amino acid residues essential for reconstitutive activity of subunit IV of the cytochrome bc_1 complex from *Rhodobacter sphaeroides*, Biochim. Biophys. Acta 1757 (2006) 1561–1567.
[11] Y. Yin, S.C. Tso, C.A. Yu, L. Yu, Effect of subunit IV on superoxide generation by *Rhodobacter sphaeroides* cytochrome bc_1 complex, Biochim. Biophys. Acta 1787 (2009) 913–919.
[12] J. Sun, B.L. Trumpower, Superoxide anion generation by the cytochrome bc_1 complex, Arch. Biochem. Biophys. 419 (2003) 198–206.
[13] I. Forquer, R. Covian, M.K. Bowman, B.L. Trumpower, D.M. Kramer, Similar transition states mediate the Q-cycle and superoxide production by the cytochrome bc_1 complex, J. Biol. Chem. 281 (2006) 38459–38465.
[14] S. Dröse, U. Brandt, The mechanism of mitochondrial superoxide production by the cytochrome bc_1 complex, J. Biol. Chem. 283 (2008) 21649–21654.
[15] D.-W. Lee, N. Selamoglu, P. Lanciano, J.W. Cooley, I. Forquer, D.M. Kramer, F. Daldal, Loss of a conserved tyrosine residue of cytochrome *b* induces reactive oxygen species production by cytochrome bc_1, J. Biol. Chem. 286 (2011) 18139–18148.
[16] L. Esser, M. Elberry, F. Zhou, C.A. Yu, L. Yu, D. Xia, Inhibitor-complexed structures of the cytochrome bc_1 from the photosynthetic bacterium *Rhodobacter sphaeroides*, J. Biol. Chem. 283 (2008) 2846–2857.
[17] C.A. Yu, L. Yu, Syntheses of biologically active ubiquinone derivatives, Biochemistry 21 (1982) 4096–4101.
[18] M.W. Mather, L. Yu, C.A. Yu, The involvement of threonine 160 of cytochrome *b* of *Rhodobacter sphaeroides* cytochrome bc_1 complex in quinone binding and interaction with subunit IV, J. Biol. Chem. 270 (1995) 28668–28675.
[19] H. Tian, L. Yu, M.W. Mather, C.A. Yu, The involvement of serine 175 and alanine 185 of cytochrome *b* of *Rhodobacter sphaeroides* cytochrome bc_1 complex in interaction with iron–sulfur protein, J. Biol. Chem. 272 (1997) 23722–23728.
[20] H.W. Ma, S. Yang, L. Yu, C.A. Yu, Formation of engineered intersubunit disulfide bond in cytochrome bc_1 complex disrupts electron transfer activity in the complex, Biochim. Biophys. Acta 1777 (2008) 317–326.
[21] J.A. Berden, E.C. Slater, The reaction of antimycin with a cytochrome *b* preparation active in reconstitution of the respiratory chain, Biochim. Biophys. Acta 216 (1970) 237–249.
[22] Y. Hatefi, J.S. Rieske, The preparation and properties of DPNH–cytochrome *c* reductase (complex I–III of the respiratory chain), Methods Enzymol. 10 (1967) 225–231.
[23] S.B. Hunter, W.F. Bibb, C.N. Shih, A.F. Kaufmann, J.R. Mitchell, R.M. McKinney, Enzyme-linked immunosorbent assay with major outer membrane proteins of *Brucella melitensis* to measure immune response to *Brucella* species, J. Clin. Microbiol. 24 (1986) 566–572.
[24] M. Nakano, Determination of superoxide radical and singlet oxygen based on chemiluminescence of luciferin analogs, Methods Enzymol. 186 (1990) 585–591.
[25] A. Denicola, J.M. Souza, R.M. Gatti, O. Augusto, R. Radi, Desferrioxamine inhibition of the hydroxyl radical-like reactivity of peroxynitrite: role of the hydroxamic groups, Free Radical. Biol. Med. 19 (1995) 11–19.
[26] X. Gong, L. Yu, D. Xia, C.A. Yu, Evidence for electron equilibrium between the two hemes b_L in the dimeric cytochrome bc_1 complex, J. Biol. Chem. 280 (2005) 9251–9257.
[27] K. Hofmann, W. Stoffel, TMbase — a database of membrane spanning proteins segments, Biol. Chem. Hoppe Seyler 374 (1993) 166.
[28] A. Krogh, B. Larsson, G. von Heijne, E.L.L. Sonnhammer, Predicting transmembrane protein topology with a hidden Markov model: application to complete genomes, J. Molecular Biology 305 (2001) 567–580.
[29] Y. Zhang, Template-based modeling and free modeling by I-TASSER in CASP7, Proteins 69 (2007) 108–117.
[30] K. Xiao, X. Liu, C.A. Yu, L. Yu, The extra fragment of the iron–sulfur protein (residues 96–107) of *Rhodobacter sphaeroides* cytochrome bc_1 complex is required for protein stability, Biochemistry 43 (2004) 1488–1495.
[31] Y. Yin, S. Yang, L. Yu, C.A. Yu, Reaction mechanism of superoxide generation during ubiquinol oxidation by the cytochrome bc_1 complex, J. Biol. Chem. 285 (2010) 17038–17045.